

# A New Probe for Measuring the Gas-Liquid Interface Profile in Horizontal Two-Phase Flows

Emerson dos Reis

[emersonr@fem.unicamp.br](mailto:emersonr@fem.unicamp.br)

Leonardo Goldstein Júnior

School of Mechanical Engineering

State University of Campinas

Laboratory of Thermal Processes and Environment Engineering

13083-970 Campinas, S. P., Brazil

[leonardo@fem.unicamp.br](mailto:leonardo@fem.unicamp.br)

**Abstract.** The measurement of the capacitance between two thin electrodes mounted around the external surface of a dielectric pipe is used to determine the profile of long bubbles in horizontal two-phase flows. This approach has some advantages over the traditional parallel wire technique: it is not intrusive, the presence of impurities dissolved in the liquid phase has no influence on the probe response, and it is applicable to very low electrical conductivity fluids, such as oils and deionized water. The static calibration of the new probe was performed using an apparatus built with a micrometer. The measurement uncertainty was calculated as  $\pm 0.32$  mm in a plexiglas pipe with 34 mm diameter. Dynamic tests with air-water two-phase flows were performed in a horizontal pipe, 5m long, and the results showed the new probe to be appropriate for application in the study of the stratified smooth, stratified wavy, plug and slug flow patterns.

**Keywords.** Capacitance Probe, Liquid Thickness Measurement, Long Bubble Profile.

## 1. Introduction

The determination of parameters such as the profile of long bubbles is essential to the study of the distribution of phases and to the calculation of the pressure drop of a slug flow in horizontal pipes.

The most common technique used to measure the profile of long bubbles – or the thickness of the liquid film –, is the parallel wire probe. This technique is based on the electrical conductance between two electrodes, shaped as wire, mounted perpendicularly to the fluids interface, as shown in Figure 1. The conductance between the wire probes is proportional to the thickness of the liquid film in the pipe, due to the difference between the liquid and the gas electrical conductivities.

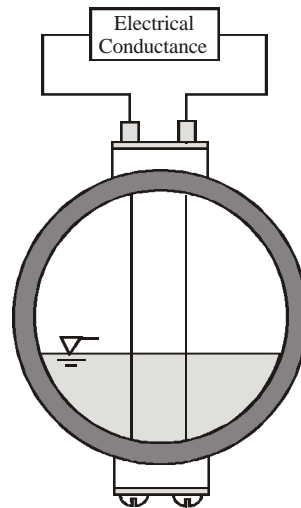


Figure 1. Parallel wire probe

Several authors studied the liquid film measurement technique using parallel wire probes, as Brow *et al.*, 1978; Koskie *et al.*, 1989; Kang and Kim, 1992; Lacy and Dukler, 1994; Shi and Kocamustafaogullari, 1994; Wong and Ooi, 1996; and Wong and Ooi, 1996b. The technique is intrusive and requires special care when assembling the system wires, which must have small diameter (0.5 mm or less) to reduce to a minimum its effect over the fluid flow. Even so, small gas bubbles can attach to the viscous wake region behind the wires, causing distortion on the system response (Koskie *et al.*, 1989). At the same time, liquid attachment between the two wires near the tube top perimeter may occur due to surface tension, limiting the probe resolution due to its impact on the conductivity between the wires. Other disadvantage of the technique is the electric conductivity dependence on the liquid temperature and on the amount of

impurities, such as mineral salts, dissolved in the liquid phase. Therefore, a compensation technique is required (Wong and Ooi, 1996). In addition, when deionized water is used, the electrical conductivity is very low and the parallel wire technique becomes inadequate

These probes can also be employed in studying flow regime identification and characterization through application of the Probability Density Function - PDF (Costigan and Whalley, 1997; King *et al.*, 1998; Lowe and Kazkallah, 1999, and Reis, 2003).

In this paper, it is presented an alternative and non-intrusive technique to measure the profile of long bubbles. This technique is based on the measurement of the capacitance between two electrodes mounted around the external surface of a dielectric material tube, and was developed to overcome the problems of the parallel wire technique.

## 2. Probe Description

The measurement device is composed of a capacitive electrode system, a sinusoidal signal source and a capacitance transducer circuit, as shown in Fig. 2. There are one sensing electrode (black), connected to the capacitance transducer, and one source electrode (dark gray), connected to the sinusoidal signal source. The sensing electrode has a small width and allows that only the liquid inside the internal volume limited by the sensing electrode affects the response of the capacitance transducer. Two guard electrodes, mounted very close to the sensing electrode (0.5 mm), avoid distortion of the electric field near its lateral borders, the so-called border effect (Reinecke and Mewes, 1996). The electric fields between the sensor electrode and the guard electrodes are null, due to the virtual ground condition imposed during the design of the capacitance transducer circuit (Yang, 1994). The smaller sensing electrode width will bring the system response closer to the liquid height on the tube cross section area. This is desirable in the measurement of waves that frequently occur in the gas-liquid flow interface. The technique limitation depends on the sensibility and on response time delay of the capacitance transducer circuit. Reis (2003) developed a transducer circuit suitable for this application, and evaluated the transducer sensibility as 7.0 mV/fF, with a response time delay of about 6 ms.

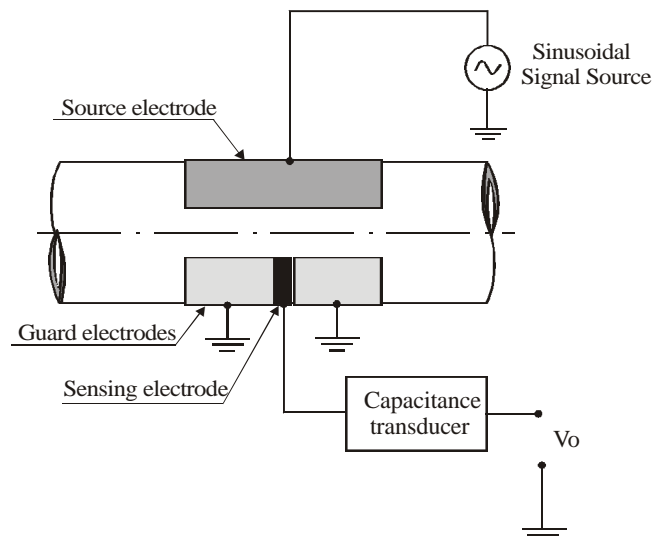


Figure 2. Thin electrode capacitance probe



Figure 3. External view of the primary capacitive system

Figures 3 and 4 show the electrodes system assembly, with an external aluminum guard screen and some constructive details.

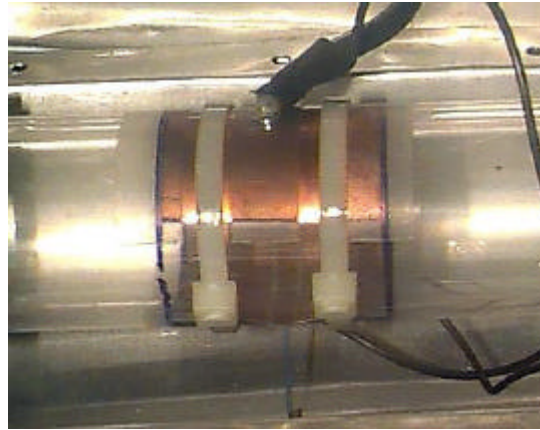


Figure 4. View of the electrode system

### 3. Probe Static Performance and Calibration

The static performance of the system was evaluated using the device schematically shown in Fig. 5. It is composed of a horizontal tube, plugged in both extremities, and divided in two parts: a rotating test section, with an angle indicator, and a static section, with a micrometer and two liquid taps on the bottom of the tube perimeter. A nylon joint with o-rings allowed a rotating movement between the sections. The base has four screws to adjust its horizontal level. The liquid film thickness was measured with a micrometer, with a range from 25 to 50 mm, and a minor scale division equals to 0.01 mm.

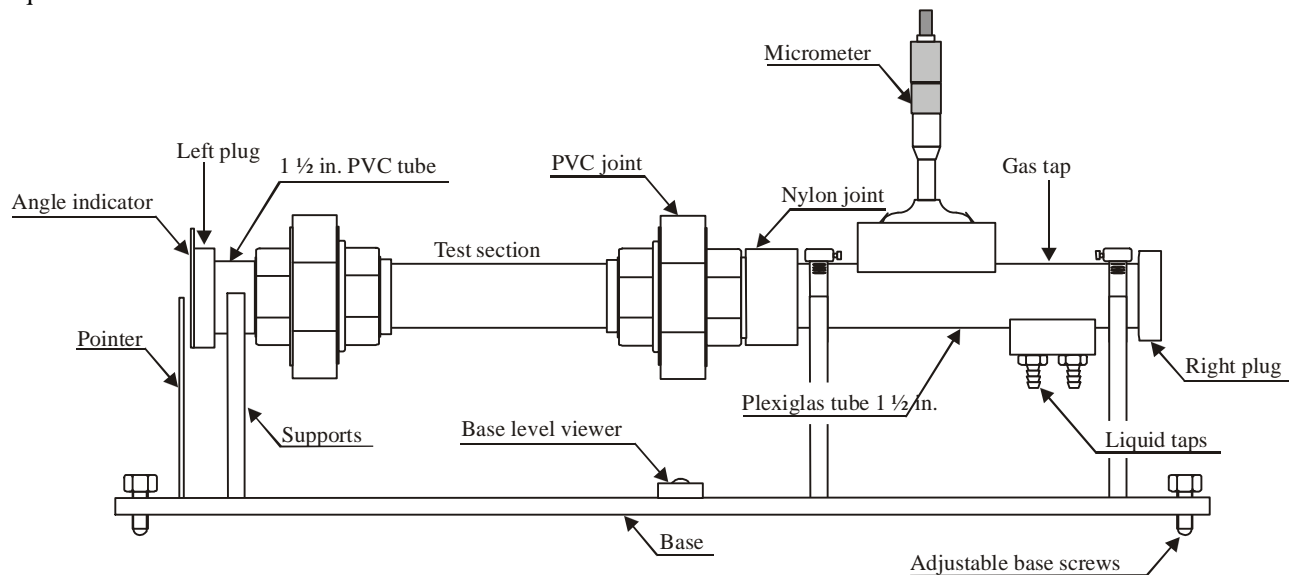


Figure 5. Static calibration device

Some parameters, such as the position of the assembly in relation to gravity, and the sensing electrode width, have influence on the measurement system sensibility and on the probe resolution, and are important in the electrodes system design.

Two different mounting positions of the electrodes relative to gravity are shown in Fig. 6. The mounting angle  $\beta$  is equal to  $0^\circ$  in the vertical condition and to  $90^\circ$  in the horizontal condition. In the horizontal condition there are two possible positioning schemes of the sensing and the source electrodes, with the sensing electrode on the upper or on the lower part of the tube perimeter. In this work, the experimental tests were performed for the horizontal case ( $\beta = 90^\circ$ ), with the sensing electrode mounted only on the tube top perimeter. Reis (2003) made a theoretical study of the electrodes system using 2D Finite Element Method modeling. He studied the system response for both electrodes mounting schemes and the same system geometry discussed below.

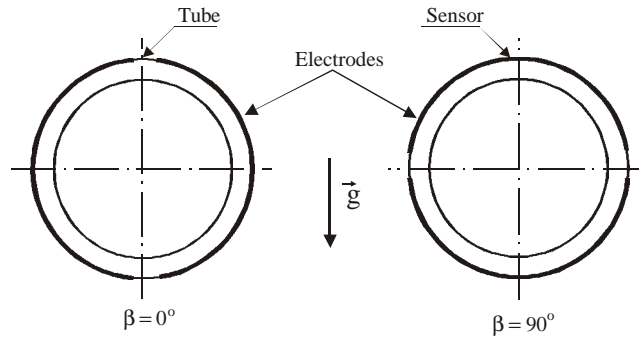


Figure 6. Mounting positions of the electrodes in relation to gravity

Figure 7 shows the top view of the system of electrodes mounted on a plexiglas tube. Two sensing electrode widths, 3 and 5 mm, were studied, with the other dimensions as indicated in Fig. 8 and Table 1.

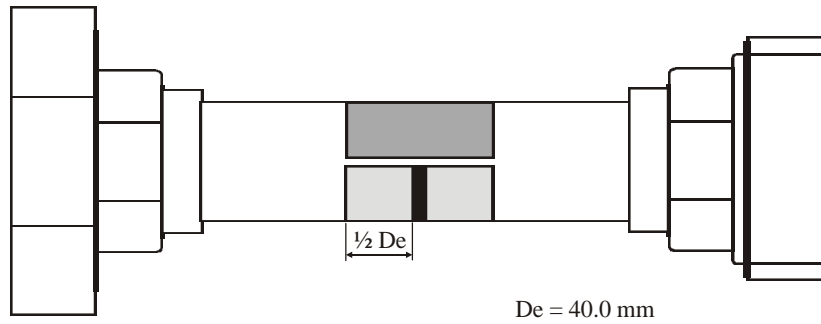


Figure 7. Electrodes mounted on the plexiglas tube

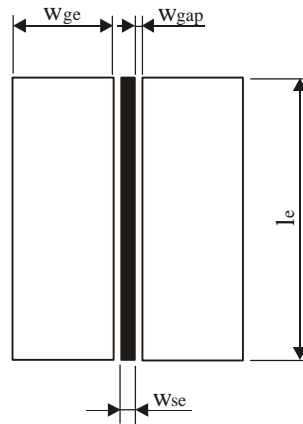


Figure 8. Electrode Parameters

Table 1. Electrode Dimensions (in mm)

$W_{se}$	$W_{ge}$	$W_{gap}$	$W_{fe}$	$l_e$
5.0	20.0	0.5	46.0	61.0
3.0	20.0	0.5	44.0	61.0

Several electrical voltages  $V_o$  were measured in the transducer output using the calibration apparatus shown in Fig. 5. They correspond to several liquid thickness  $h_L$  in the tube. Both sensing electrode widths were tested, with both the mounting angles  $\beta$ , shown in Fig. 8.

Figure 9 shows the 3 mm sensing electrode system response from  $h_L = 0$  mm, when the tube was filled with gas (atmospheric air), to  $h_L = 34.0$  mm, when the tube was filled with liquid (clear water). The mounting scheme with  $\beta = 0^\circ$  produced a linear response for  $h_L > 5$  mm, while with  $\beta = 90^\circ$  the system response exhibited a non-linear characteristic. Since linearity is always desirable in instrumentation,  $\beta = 0^\circ$  was chosen as the mounting electrodes angle to be used in the probe experimental dynamic tests, discussed in the next section.

Another important consideration in Fig. 9 is the presence of blank intervals due to the lack of data. This is observed in two data regions:  $h_L < 5$  mm and  $h_L > 25$  mm. In the first region, it is due to the effect of surface tension in the gas-liquid interface, which produces a non-uniform liquid level across the tube section area. In the second region, when  $h_L > 25$  mm, the blank interval is due to the micrometer measurement range upper limit of 25 mm, that is not enough to cover the entire tube diameter of 34.0 mm.

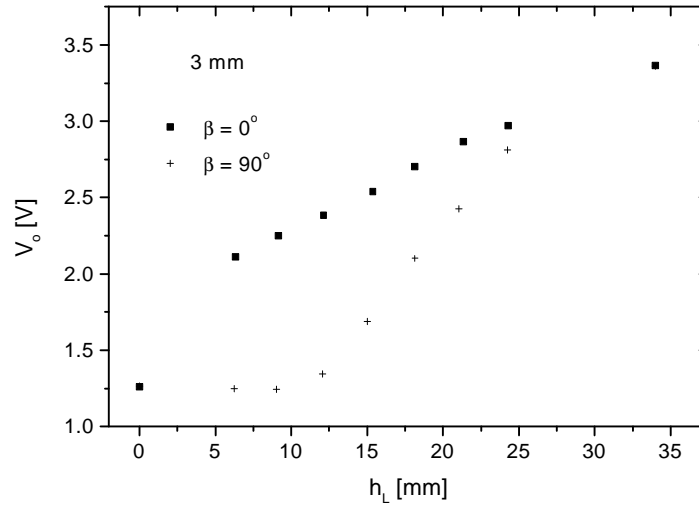


Figure 9. Capacitance transducer response for the 3 mm sensing electrode system

Figure 10 shows the transducer output voltage  $V_o$  versus the liquid film thickness  $h_L$  for both the 3 and 5 mm sensing electrode systems, mounted vertically with  $\beta = 0^\circ$ . The angular coefficient of the response of the 5 mm sensing electrode system is greater than that of the 3 mm sensing electrode system, which means that the 5 mm electrode system has greater sensibility. Nonetheless, one would expect that a smaller width would allow greater spatial resolution, providing results more representative of the tube cross section. Based on this, the 3 mm sensing electrode was chosen to be used in the dynamic tests which were executed.

It can be observed that the linear response has an interruption at  $h_L = 5$  mm, a phenomenon which was also experienced by Reis (2003) in a theoretical 2D Finite Element Method study. The study points the concave geometry of the electrode as the main cause for that. As was discussed there, it would be possible to obtain a linear response in the entire range, from 0 to the tube diameter, if the electrodes length  $l_e$  was altered accordingly.

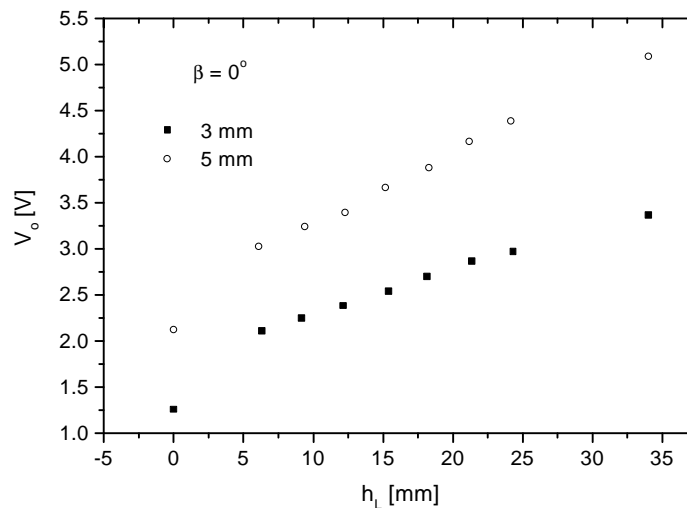


Figure 10. Capacitance transducer response for the 3 and 5 mm sensing electrode systems

Figure 11 shows the calibration curve for the 3 mm sensing electrode system, with  $\beta = 0^\circ$ . Eighteen data points were taken 9 from the lower to the upper limit of the range and 9 from the upper to the lower limit with 16 points within the linear curve region. The measurement uncertainty was determined as  $\pm 0.521$  mm, or  $\pm 1.532\%$  of full scale. The bias measurement uncertainty of the micrometer was  $\pm 0.01$  mm, and the precision uncertainty determined as  $\pm 0.245$  mm, with the student coefficient  $t_{95}$  equal to 2.120.

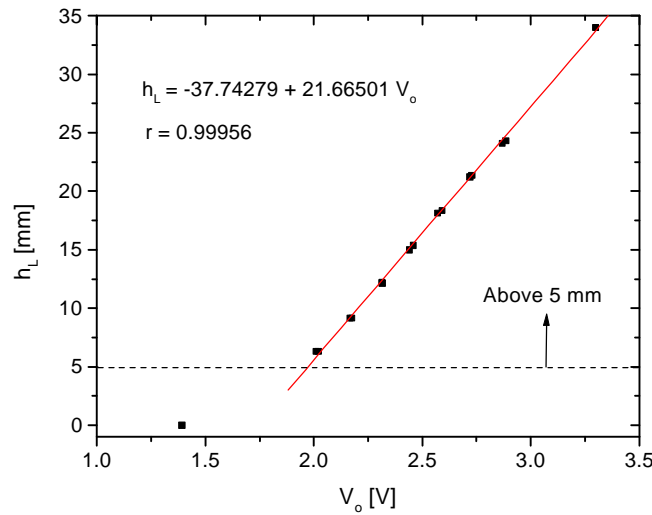


Figure 11. System calibration curve

#### 4. Probe Dynamic Performance

Static calibration makes possible to evaluate only the static performance of the metering system. The dynamic performance was evaluated using an experimental apparatus designed by Reis (2003), shown in Fig. 12. The elongated air bubbles were produced in a horizontal 5 m long (140 hydraulic diameters), 34 mm internal diameter plexiglas pipe, and the bubbles profiles were measured with the probe.

When liquid water is flowing into the pipe, pressurized air is injected through a solenoid valve installed at the mixing point, located 5 m upstream of the measurement probe. The water flow rate,  $Q_L$ , was adjusted using a control valve and measured with a turbine meter (range from 3 to 45 l/min and a calibrated measurement uncertainty equals to  $\pm 0.25$  l/min).

It was used a data acquisition system composed of an AT-MIO-16E10 board, a connections block, and the Labview 5.0, by National Instruments<sup>TM</sup>. For each test, two time intervals were adjusted in the data acquisition and control program. One for the air injection period, during which the solenoid valve VS stays opened, and the other for the time the program will wait before starting data acquisition. Other inputs to the acquisition program were the number of samples and the samples acquisition rate (the acquisition time is equal to the sample number divided by the sampling rate). The acquisition time must be sufficient to allow registration of the whole elongated air bubble, and the time delay is necessary so that the bubble reaches the probe system while the bubble profile develops after the mixing point.

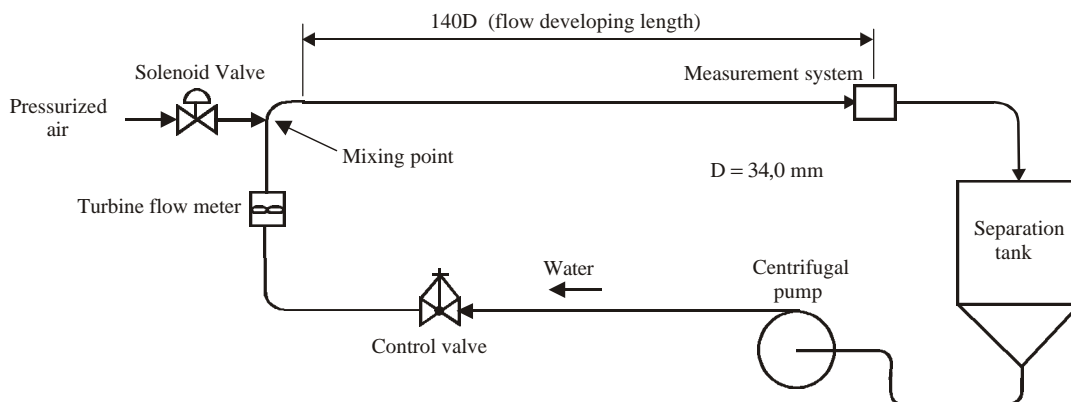


Figure 12. Experimental apparatus schematic

The nominal water flow rates chosen for the tests were 20 l/min and 36 l/min, with a time delay of about 4.0 s, an air injection duration of 0.5 s, at an air injection pressure of 0,5 kgf/cm<sup>2</sup>. Tests were performed with both the 3 and 5 mm widths sensing electrode systems, and in both mounting positions,  $\beta = 0^\circ$  and  $\beta = 90^\circ$ . It is important to observe that in both tests the liquid Reynolds number,  $Re$ , was greater than 2200 (14570 and 26226, respectively), characterizing turbulent flows. According to Incropera and DeWitt (1996), the minimum development length for turbulent flows in pipes is equal to  $60 D$ . A length of  $140 D$  was available in the experimental apparatus before the test section, which was shown adequate to guarantee the long bubble profile development. On the other hand, the bubble air injection causes flow transients and oscillations in the incoming probe flow, mainly because of the air compressibility.

The test points were characterized by the Froude number,  $Fr_U$ , defined by Netto *et al.* (1999) as

$$Fr_U = \frac{U}{\sqrt{gD}} \quad (1)$$

where  $g$  is the gravity acceleration and  $U$  is the mean velocity of the liquid flow in the pipe:

$$U = Q_L / A,$$

and  $A$  is the pipe cross section area.

Netto *et al.* (1999) studied the elongated bubbles as a function of the fluid properties (air and water) and the Froude number. They reported the elongated bubbles as having a short nose, a wavy air-water interface, with constant wave length and decreasing amplitude, and a bubble tail finished with an abrupt liquid level change, or hydraulic jump, for the lower fluid velocities,  $Fr_U < 1$ . After the hydraulic jump, the liquid did not reach the pipe upper wall surface, but created a decreasing prolonged thin tail behind the bubble. An interesting aspect of the wavy interface is that it stays frozen relative to the bubble, during the bubble movement. On the other hand, for  $Fr_U > 1$ , that is, if the Froude number increases, the bubble nose becomes longer, the amplitude of the waves in the air-water interface decreases, and the tail after the hydraulic jump is short.

The changing characteristics of the elongated bubble profile with the Froude number were utilized in this work to evaluate the dynamic response of the new probe, so that, by varying the liquid flow rate  $Q_L$ , prolonged bubbles were produced, with several shapes, as described above. An alternative approach to verify the dynamic response of the system would be its direct comparison with the response of another meter type, in such a way that both are traversed by the same elongated bubble. A possibility would be, for example, a comparison with the parallel wire probe performance described in the beginning of the paper.

Figures 13 - 16 present the electrical voltage  $V_o$  at the capacitance transducer, obtained during the elongated bubble passage through the system electrodes, normalized by the initial electrical voltage detected at time  $t = 0$  s, as a function of  $t$  in the abscissa axis. The tests were performed in several fluid flow conditions, using both sensing electrode systems, such that the black and red lines represent the signals from the 3 and 5 mm electrode systems, respectively. For both electrode systems, the signals were acquired at the same flow condition and with the same mounting scheme, but at different test times, so that the elongated bubbles are similar but not the same.

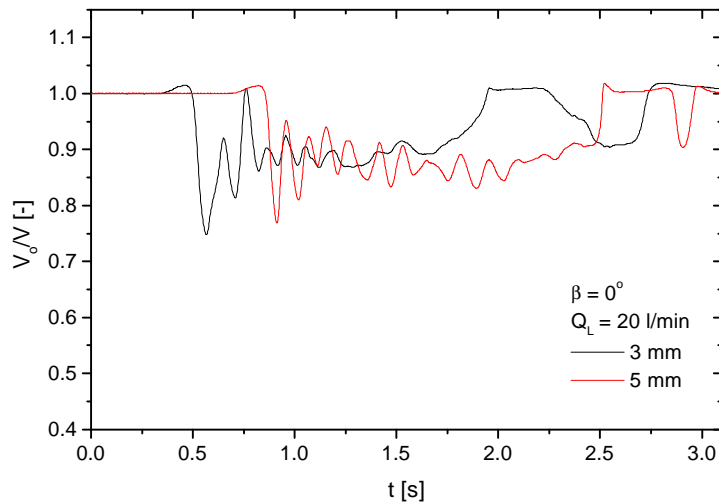


Figure 13. Capacitance transducer voltage ratio response, Long Bubble Profile,  $Fr_U = 0.637$  and  $\beta = 0^\circ$

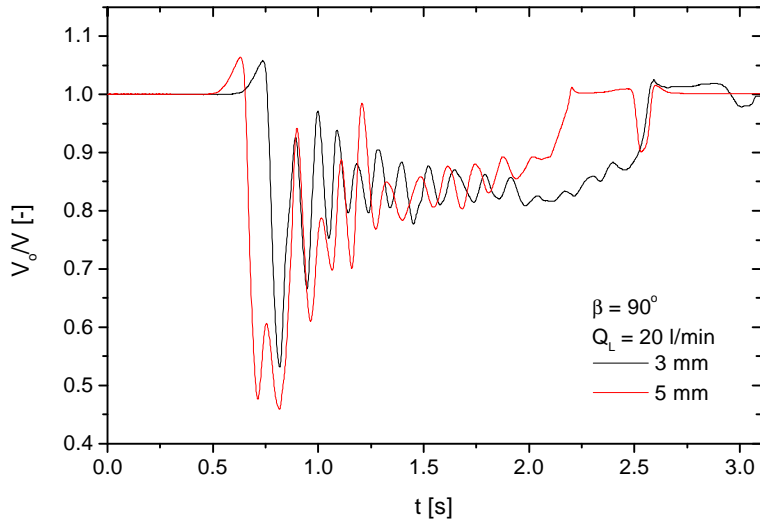


Figure 14. Capacitance transducer voltage ratio response  
 Long bubble profile,  $Fr_U = 0.637$  and  $\beta = 90^\circ$

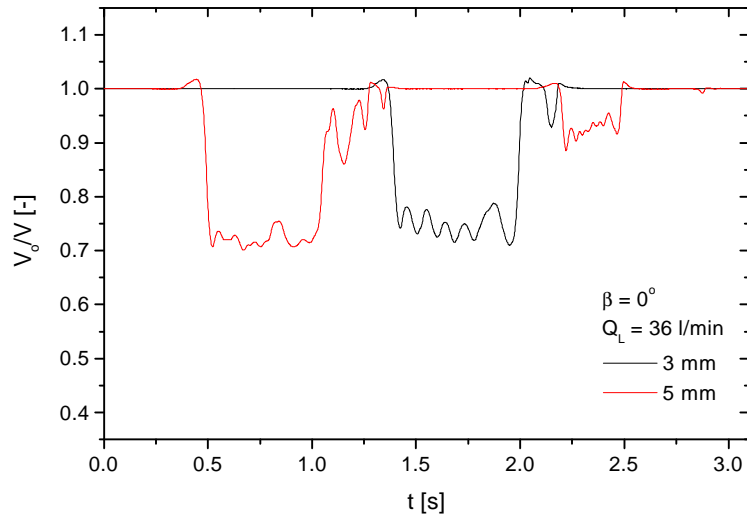


Figure 15. Capacitance transducer voltage ratio response  
 Long bubble profile,  $Fr_U = 1.146$  and  $\beta = 0^\circ$

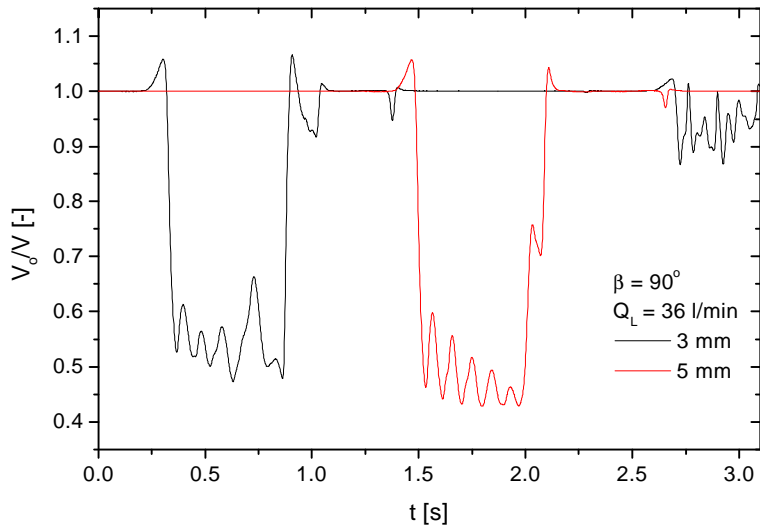


Figure 16. Capacitance transducer voltage ratio response  
 Long bubble profile,  $Fr_U = 1.146$  and  $\beta = 90^\circ$



The first point to be noted refers to the choice of the mounting angle of the electrodes,  $\beta = 0^\circ$  or  $\beta = 90^\circ$ . The linear or non-linear response of the measurement system depends on the mounting angle, as discussed in the previous item, with consequences on the output voltage graphs. The comparison of Figs. 13 and 14, and of Figs. 15 and 16 shows different output voltage signals when  $\beta = 0^\circ$  and  $\beta = 90^\circ$ , such that the signal oscillations for  $\beta = 90^\circ$  have a greater amplitude than for  $\beta = 0^\circ$ . It can also be observed that when the electrodes are mounted vertically ( $\beta = 0^\circ$ ), the output voltage  $V_0$  is proportional to the liquid film thickness  $h_L$ , which is an advantage, mainly during test execution.

A second point refers to the observation that the 3 and 5 mm wide sensing electrodes produced similar voltage signal ratios, indicating that the tests were not capable of identifying if the response signals depend on the sensing electrode width or not, what suggests that further tests should be performed with larger sensing electrode widths, such as 10 mm or more.

The figures show the presence of “jumps” in the output voltage signals near before the bubble nose and, sometimes, in its tail. These jumps do not represent a physical reality, since to  $V_0/V > 1$ , it would correspond  $h_L > D$ , a situation which is impossible to occur. A possible explanation for this phenomenon could be “over shoot” (Smith, 1999), related to the response of the electronic filter that exists in the capacitance transducer output. However, a low-pass Bessel filter type, that does not present over shoot, was used, and the phenomenon persisted, as shown in the figures. Another possible explanation for the phenomenon could be a distortion in the electric field between the electrodes, caused by the nose bubble advance. The same would happen close to the tail, after the bubble passage. A 3D modeling of the electrodes, using the Finite Element Method, for example, should be able to explain this effect, to be verified in a future work. Finally, the voltage jumps in the capacitance transducer output are minimized with higher flow velocities. The higher frequency signals are cut out by the electronic low-pass filter, at a cutoff frequency of about 200 Hz.

## 5. Measurement of the Gas-Liquid Interface Profile

Figures 17 and 18 show the signals produced by the new probe for three air-water flow patterns, with gas  $u_{GS}$  and liquid  $u_{LS}$  superficial velocities, which can be identified as: wavy stratified and slug flows, respectively. Physically coherent signals can be observed in all these figures, which allow the characterization of these horizontal two-phase flows.

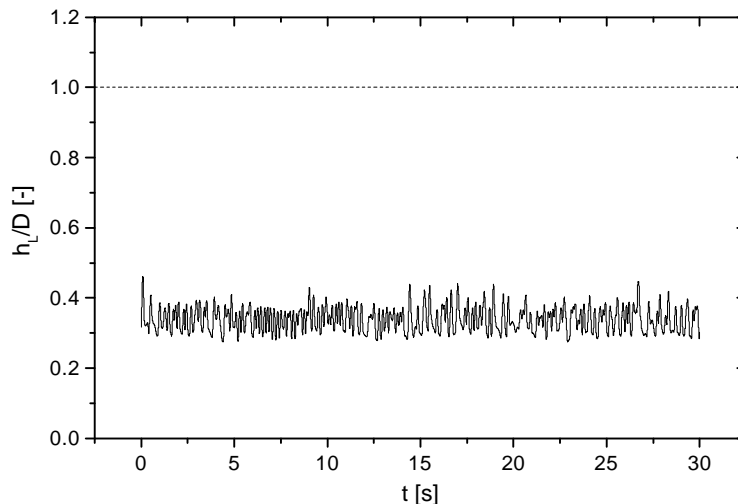


Figure 17. Measurement system signal for wavy air-water flow in a 34 mm pipe,  
 $u_{LS} = 0,080$  m/s e  $u_{GS} = 3,225$  m/s

It can be observed in Fig. 18 that the signals previously filtered do not touch the dotted line representing the tube upper surface, as the liquid slugs pass through. This fact is associated to the small gas bubbles which are present in the slugs, causing a reduction of the probe response. These results show that an effective measurement of the liquid film thickness can be achieved in mixed gas-liquid flow conditions.

## 6. Conclusion and Remarks

In this paper, a new non-intrusive technique was presented, to be applied in dedicated two-phase flow experimental apparatuses, to measure the profile of long bubbles in horizontal two-phase flows. The technique is based on the measurement of the capacitance between two thin electrodes mounted around the external surface of a dielectric material tube.

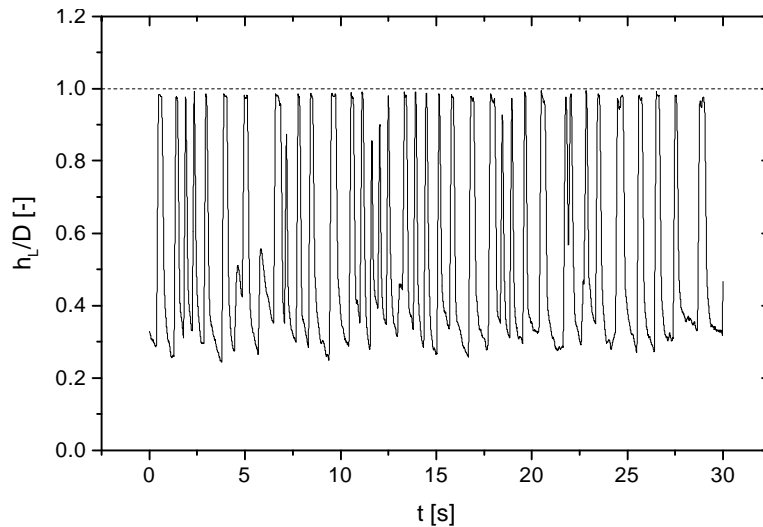


Figure 18. Measurement system signal for slug air-water flow in a 34 mm pipe,  
 $u_{LS} = 0.788$  m/s e  $u_{GS} = 1.392$  m/s

The static tests showed that the system has a linear response when the electrodes are installed in a vertical mounting scheme ( $\beta = 0^\circ$ ). The 5 mm wide sensing probe presented greater sensibility than the 3 mm electrode. Otherwise, the spatial resolution of the 3 mm system had to be 40% greater. The static calibration showed a linear probe response in the range from 5 to 34 mm, corresponding to 15% to 100% of the full scale.

The dynamic tests showed the existence of jumps in the output voltage response of the system, attributed to the distortion of the electric field due to the fast changes in the level of the liquid flowing through the pipe. This effect should be minimized with the utilization of a digital filter in the data processing phase.

In a general way, the probe has shown to be suitable to study gas-liquid flows in round tubes, allowing the application of signal analysis techniques to obtain several flow characteristics.

## 7. Acknowledgement

The support of FAPESP – Fundação de Amparo à Pesquisa do Estado de São Paulo, Brazil, is deeply appreciated.

## 8. References

- Brown, R. C., Andreussi, P., Zanelli, S., 1978, "The use of wire probe for the measurement of liquid film thickness in annular gas-liquid flows", *The Canadian Journal of Chemical Engineering*, Vol. 56.
- Costigan, G., Whalley, P. B., 1997, "Slug flow regime identification from dynamic void fraction measurements in vertical air-water flows", *International Journal of Multiphase Flow*, Vol. 23, n. 2, pp.263-282.
- Kang, H. C., Kim, M. H., 1992, "The development of flush-wire probe and calibration method for measuring liquid film thickness", *International Journal of Multiphase Flow*, Vol. 18, n. 3, pp. 423-437.
- King, M. J. S., Hale, C. P., Lawrence, C. J., Hewitt, G. F., 1998, "Characteristics of flowrate transients in slug flow", *International Journal of Multiphase Flow*, Vol. 24, pp. 825-854.
- Koskie, J. E., Mudawar, I., Tiederman, W. G., 1989, "Parallel-wire probes for measurement of tick liquid films", *International Journal of Multiphase Flow*, Vol. 15, n. 4, pp. 521-530.
- Lacy, C. E., Duckler, A. E., 1994, "Flooding in vertical tubes - I Experimental studies of the entry region", *International Journal of Multiphase Flow*, Vol. 20, n. 2, pp. 219-233.
- Lowe, D. C., Rezkallah, K. S., 1999, "Flow regime identification in microgravity two-phase flows using void fraction signals", *International Journal of Multiphase Flow*, Vol. 25, pp. 433-457.
- Reinecke, N., Mewes, D., 1996, "Recent developments and industrial/research applications of capacitance tomography", *Measurement Science and Technology*, Vol. 7, n. 3, pp. 233-246.
- Reis, E. dos. 2003, *Estudo do escoamento pistonado horizontal ar-água em tubulações com ramificação "T"*: School of Mechanical Engineering, State University of Campinas, 2003. PhD Thesis in portuguese.
- Shi, J., Kocamustafaogullari, G., 1994, "Interfacial measurements in horizontal stratified flow patterns", *Nuclear Engineering and Design*, Vol. 149, pp. 81-96.
- Wong, T. N., Ooi, K. T., 1996a, "Performance of parallel-wire depth probe", *International Communication of Heat and Mass Transfer*, Vol. 23, n. 7, pp. 1003-1009.
- Wong, T. N., Ooi, K. T., 1996b, "A calibration technique for a parallel-wire depth probe with conductivity compensation", *Experiments in Fluids*, Vol. 20, pp.429-432.